

# Design method and behavior factor for steel frames with buckling restrained braces

Melina Bosco<sup>\*,†</sup> and Edoardo M. Marino

*Department of Civil and Environmental Engineering, University of Catania, V.le A. Doria, 6, 95125 Catania, Italy*

## SUMMARY

Buckling restrained braces (BRBs) are very effective in dissipating energy through stable tension–compression hysteretic cycles and have been successfully experimented in the seismic protection of buildings. Their behavior has been studied extensively in the last decades and today the level of performance guaranteed by these devices and the technological constraints that have to be fulfilled to optimize their behavior are well known. Furthermore, several companies in the world have developed their own BRBs and are now producing them. In spite of this, many seismic codes (for instance, the EuroCode 8) do not stipulate provisions for the design and construction of earthquake-resistant structures equipped with BRBs. This discourages the structural engineering community from using these devices and seriously limits their use in structural applications. In this paper a procedure for the seismic design of steel frames equipped with BRBs is proposed. Furthermore, the paper presents a numerical investigation aimed at validating this design procedure and proposing the value of the behavior factor  $q$  that should be used for this structural type. To this end, a set of frames with BRBs is first designed by means of several values of  $q$ . Then, the obtained frames are subjected to a set of accelerograms compatible with the elastic response spectrum considered in design. The seismic response of the frames is determined by nonlinear dynamic analysis and represented in terms of the ductility demand of BRBs and the internal force demand of nondissipative members (beams and columns). Finally, the largest value of  $q$  that leads to acceptable seismic performance of the analyzed frames is assumed as adequate. The value of  $q$  is given in the paper as a continuous function of the assumed ductility capacity of the BRBs. Copyright © 2012 John Wiley & Sons, Ltd.

Received 8 June 2012; Revised 1 October 2012; Accepted 3 October 2012

**KEY WORDS:** BRB; chevron braced frame; steel structure; behavior factor; seismic code

## 1. INTRODUCTION

The seismic design of structures is generally performed by applying equivalent static forces, which are reduced with respect to the elastic ones to take into account the expected ductility of the structure. To this aim, seismic codes suggest reducing the seismic force by means of the behavior factor  $q$ . A proper value of  $q$  is provided with reference to several structural types. Among others, the EuroCode 8 (EC8) [1] stipulates rather small values of the behavior factor  $q$  for braced frames ( $q=2.5$  for chevron braced frames) because of the low dissipation capacity of conventional steel braces. This determines a large required strength.

To overcome the low dissipation capacity of conventional steel braces, a new dissipative brace was developed. This device, named buckling restrained brace (BRB), dissipates energy through stable tension–compression hysteretic cycles. Research on BRBs was first carried out in Japan; later on various types of BRBs were developed mainly in Asia and, after the 1994 Northridge earthquake, in the United States. An exhaustive review of the state of the art of BRBs can be found in [2–4]. BRBs

<sup>\*</sup>Correspondence to: Melina Bosco, Department of Civil and Environmental Engineering, University of Catania, V.le A. Doria, 6, 95125 Catania, Italy.

<sup>†</sup>E-mail: mbosco@dica.unict.it

have been successfully experimented in Japan in the seismic protection of buildings, where they are used as hysteretic dampers combined with moment-resisting frames. In some other countries BRBs are used as a variation of braced frames, that is, BRBs are inserted in low redundant frames in which beams are connected to columns by means of pinned joints. Some studies have pointed out that the low post-yield stiffness of BRBs may cause buckling restrained braced frames to exhibit large maximum and residual drifts [5, 6]. These studies have also remarked that the adoption of dual systems reduces appreciably the residual story drift and slightly the maximum drift.

Although many studies have pointed out the remarkable ductility of BRBs, some seismic codes, for instance EC8, do not provide the value of the behavior factor to adopt in the design of frames equipped with these devices. To promote the application of BRBs, the Structural Engineers Association of Northern California proposed the 'Recommended provisions for buckling restrained braced frames' [7] in which two different values of the behavior factor were suggested [8]. Specifically, a value of  $q$  equal to either 8 or 9 was proposed in the case of BRBs inserted in frames with pinned beam-to-column connections or with moment-resistant beam-to-column connections, respectively. Later on, based on this document, the 'NEHRP Recommended Provisions for Seismic Regulation for New Buildings and other Structures' (FEMA-450) [9] and the AISC 2005 'Seismic Provision for Structural Steel Buildings' [10] stipulated values of the behavior factor slightly lower and equal to either 7 or 8 in the case of pinned or moment-resistant beam-to-column connections, respectively. As pointed out in other studies [2], these values of the behavior factor are comparable to that adopted in EC8 for a high-ductility moment-resisting frame. Some studies on this topic [11–13] underline that the behavior factor for the design of buckling restrained braced frames decreases as the height of the building increases. Specifically, according to Asgarian and Shokrgozar [11], values of the behavior factor ranging from 4 to 13 can be adopted for buckling restrained braced frames designed by the Iranian National Building Code for Structural Steel Design. On the basis of this finding, which is almost independent of the type of bracing configuration, a design value of  $q$  equal to 8.35 is suggested. The behavior factors obtained by Mahmoudi and Zaree [12] with reference to different brace configurations (chevron V and X bracing) in a single bracing bay vary between 7 and 16. The results reported in the study of Kim *et al.* [13] show that although high values of  $q$  can be adopted in 4-story frames, the behavior factors obtained for structures taller than 4 stories are generally smaller than those proposed in FEMA-450 and AISC 2005. Sabelli *et al.* [14] underlined that the response of the braced frames considered in their study is not sensitive to response modification factors selected within the range of 6 and 8. According to the findings of Fahnestock *et al.* [15, 16], buckling restrained braced frames with pinned beam-to-column connections designed with a behavior factor equal to 8 performed well. Finally, according to preliminary results obtained by other authors [17, 18], proper values of the behavior factor are in the range 3.5–7.

In the opinion of the authors, the effectiveness of the suggested values of  $q$  has not been thoroughly investigated with reference to BRBs inserted within concentrically braced frames with pinned beam-to-column connections. Furthermore, the findings of literature studies are often contradictory. Finally, because different BRBs available in the market can tolerate different ductility demands before failure, the value of the behavior factor should be correlated to the available ductility of the adopted BRBs. Specifically, because the ductility of BRBs presents a variation almost continuous in a wide range, the value of the behavior factor should be given as a continuous function of the available ductility of the adopted BRBs.

In the paper, a set of steel frames equipped with BRBs in the chevron configuration is designed by means of several values of the behavior factor. The frames have different numbers of stories and are equipped with BRBs characterized by different values of the available ductility. The seismic behavior of the frames is evaluated by nonlinear dynamic analysis to select the higher value of  $q$ , which leads to frames able to fulfill the life safety performance level requirements.

## 2. CYCLIC BEHAVIOR AND MODELING OF BUCKLING RESTRAINED BRACES

The BRBs (Figure 1) are composed of a ductile steel core, which is encased over its length in a steel tube (usually a hollow structure shape) filled with concrete. The casing precludes the buckling of the steel core, which will yield in both tension and compression. A slip interface (unbonding layer) between the steel core and the surrounding concrete is provided to avoid the transfer of the axial force from the steel core

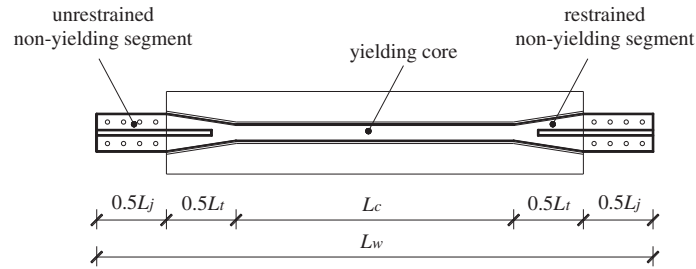


Figure 1. Components of buckling restrained brace.

to the casing and to ensure that compressive and tensile axial forces are carried by the steel core only. The projection of the yielding core is the restrained nonyielding segment. It is surrounded by the casing but it behaves elastically during cyclic loading because its cross-sectional area  $A_t$  is larger than the area  $A_c$  of the yielding segment. Finally, the brace is connected to the surrounding frame by means of the unrestrained nonyielding segment, which is the projection of the restrained nonyielding segment over the casing [3]. The area  $A_j$  of the cross-section of this segment is larger than  $A_t$ .

The cyclic behavior of BRBs has been investigated extensively in experimental studies [19–28]. Unfortunately, the results of these studies cannot be directly compared because BRBs are often arranged in different configurations and subjected to different loading protocols. Nevertheless, these tests typically show hysteretic loops having nearly ideal bilinear hysteretic shapes with kinematic and isotropic hardening. Furthermore, the axial strength of BRBs is slightly greater in compression than in tension because of friction between the core and the jacket. Different response parameters are measured during the tests: (i) the brace axial elongation and shortening  $\delta$ ; (ii) the tension strength adjustment factor  $\omega$  (ratio of the maximum tension force to the axial yielding force  $N_y$ ); and (iii) the compression strength adjustment factor  $\beta$  (ratio of the maximum compression to maximum tension force). Furthermore, two types of ductility capacity are defined and calculated: the maximum ductility capacity and the cumulative ductility capacity. The maximum ductility capacity is defined as the ratio of the BRB maximum elongation/shortening  $\delta_{\max}$  to the yielding value  $\delta_y$ . The cumulative ductility demand  $\mu_c$  is defined as

$$\mu_c = \frac{\sum \delta_{pl}}{\delta_y} \quad (1)$$

where  $\delta_{pl}$  is the BRB plastic deformation. More details on the cumulative ductility can be found in [29, 30].

As demonstrated by the experimental tests described by Merritt *et al.* [25] and by Newell *et al.* [26], maximum ductility in the range 10 to 22 can be achieved. Note that these values are lower bounds on the available ductility of BRBs because failure occurred only for a few of the tested specimens.

In this study a bilinear relation between the axial force and the brace elongation (backbone curve) is adopted to represent the BRB behavior. On the basis of the results of the above mentioned experimental tests, the post-yield stiffness ratio  $k_h$  is calibrated so that a tension strength adjustment factor equal to 1.75 corresponds to an available ductility equal to 15. The obtained value of the kinematic hardening also includes the effects of isotropic hardening. Because the BRB hardening tends to saturate at large deformations, a pure kinematic hardening can over-predict brace strength for ductility demand much larger than 15.

### 3. PROPOSED DESIGN PROCEDURE

Buckling-restrained braced frames are a special class of concentrically braced frames. Only a few of the recent seismic codes (e.g., AISC 2005) give some provisions for the design of such systems. These provisions are intended to ensure that braces are used only within their range of deformation capacity, and that yield and failure modes of other members are precluded. Other seismic codes, for example, EC8, do not specify any value of the behavior factor or any provision regarding the application of capacity design principles to beam and column members belonging to buckling

restrained braced frames. In this section a design procedure for buckling restrained braced frames arranged in the chevron configuration is proposed. The procedure is developed for EuroCode 8, but it can be easily adjusted for other codes. The braces are designed on the basis of axial forces evaluated by a modal response spectrum analysis of the frame assuming a design spectrum reduced by an assigned value of the behavior factor  $q$ . According to the capacity design principles, the design internal forces of beams and columns are obtained by the equilibrium of the frame assuming that all the braces are fully yielded and characterized by an axial deformation equal to that corresponding to the attainment of the maximum ductility capacity (fully hardened braces).

For the sake of simplicity, the modal response spectrum analysis is performed on a structural scheme in which all connections are pinned. Furthermore, the BRBs are modeled by a truss element characterized by a cross-section with an equivalent area  $A_{eq}$  equal to

$$A_{eq} = \frac{A_c}{\frac{L_j}{L_w} \frac{A_c}{A_j} + \frac{L_t}{L_w} \frac{A_c}{A_t} + \frac{L_c}{L_w}} \quad (2)$$

where  $L_c$ ,  $L_t$ ,  $L_j$  and  $L_w$  are the length of the yielding core, the restrained nonyielding segment, the unrestrained nonyielding segment, and the whole brace, respectively (Figure 1).

### 3.1. Design of the braces

The cross-sectional area of the core of the BRB is evaluated by equating the design story shear  $V_{Ed,i}$  to the lateral strength  $V_{Rd,i}$  provided by a pair of chevron BRBs, that is, to the story shear that produces the yielding of the braces

$$A_{c,i} = \frac{V_{Ed,i}}{2f_y \cos \alpha} \quad (3)$$

where  $f_y$  is the yielding stress of the BRB's core and  $\alpha$  is the angle of inclination of the brace with respect to the longitudinal beam axis.

The available ductility that BRBs should possess is evaluated on the basis of a design story drift  $\Delta u^d$ , that is, the maximum accepted story drift demand for earthquakes with the assigned probability of occurrence. The design story drift is a designer choice, although a value compatible with BRB technology must be selected. Indeed, according to the qualifying cyclic tests stipulated in AISC 2005 [10], the buckling-restraining systems have to be able to sustain deformations corresponding to two times the design story drift: the higher the values of the design story drift, the greater the available ductility that BRBs have to achieve when subjected to qualifying tests.

To evaluate the required ductility of the BRBs, the story drifts  $\Delta u_i$  produced by the design seismic forces are first calculated by means of a computer program. Because, in this study, the cross-sectional area assigned to BRBs is exactly equal to that required by the story shear, the story drifts  $\Delta u_i$  are also equal to the yielding story drifts  $\Delta u_i^y$ . If the flexural stiffness of the columns is neglected, the story drifts  $\Delta u_i$  provided by the design forces are the sum of the contributions  $\Delta u_i^b$  and  $\Delta u_i^c$  due to the axial deformations of braces and of columns, respectively (Figure 2). The two deformative contributions can be calculated as

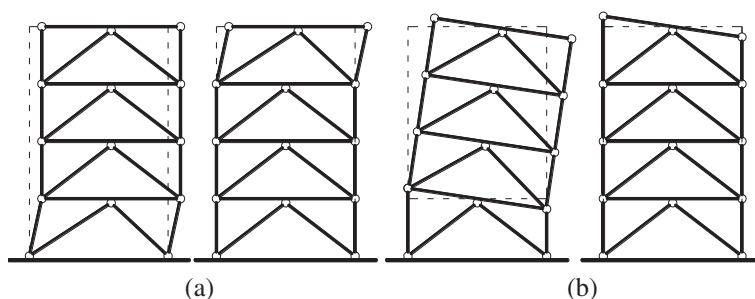


Figure 2. Deformative contributions in buckling restrained braced frames: (a) braces and (b) columns.

$$\Delta u_i^b = \frac{A_{c,i} f_y L_w}{EA_{eq,i} \cos \alpha} \quad (4a)$$

$$\Delta u_i^c = \Delta u_i - \Delta u_i^b = \Delta u_i^y - \Delta u_i^b \quad (4b)$$

As the design story drift  $\Delta u^d$  is larger than  $\Delta u_i$ , the braces undergo plastic deformations. When the yielding story drift  $\Delta u_i^y$  is exceeded, the contribution provided by the axial deformations of the columns becomes negligible. The increase of the drifts, mainly because of the plastic deformations in braces, is

$$(\mu_i - 1) \cdot \Delta u_i^b = \Delta u^d - (\Delta u_i^b + \Delta u_i^c) \quad (5)$$

where  $\mu_i$  is the required ductility of the braces. Finally, the ductility  $\mu_{\max,i}$  that the braces should possess is calculated so that the buckling-restraining system sustains deformations corresponding to 2.0 times those required by the design story drift

$$\mu_{\max,i} = 2\mu_i = 2 \frac{\Delta u_i^d - \Delta u_i^c}{\Delta u_i^b} \quad (6)$$

### 3.2. Design of beams and columns of the braced frames

With reference to chevron braced frames, seismic codes require that braces yield and dissipate energy during strong ground motions, while beams and columns have to remain elastic. According to this principle, the design internal forces of beams ( $N_{Ed}^b$ ,  $M_{Ed}^b$ ) and columns ( $N_{Ed}^c$ ) are obtained by the equilibrium of the frame at collapse and assuming that all the braces are fully yielded and hardened. The ultimate axial forces in braces in tension and in compression are equal to  $\omega N_y$  and  $\beta \omega N_y$ , respectively.

First, from the horizontal equilibrium of the beam at the  $i$ -th story, the horizontal forces  $F_i$  acting at both ends of the beam (Figure 3) are evaluated as

$$F_i = (\omega N_y + \beta \omega N_y)_i \cos \alpha - (\omega N_y + \beta \omega N_y)_{i+1} \cos \alpha \quad (7)$$

Second, by supposing that  $F_i$  are equally shared between the two ends of the beam of the  $i$ -th story (Figure 3(b)), the axial force acting on each part of the beam is calculated by the following relations:

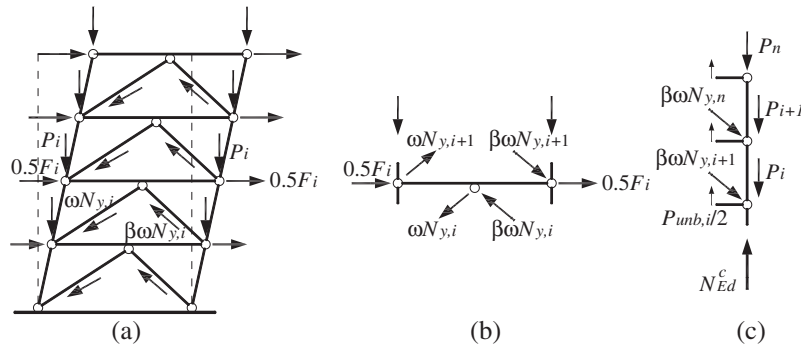


Figure 3. Evaluation of design forces in beams and columns.

$$N_{\text{Ed},i}^{\text{b}} = 0.5 F_i + (\omega N_y)_{i+1} \cos \alpha \quad (\text{compression}) \quad (8a)$$

$$N_{\text{Ed},i}^{\text{b}} = 0.5 F_i + (\beta \omega N_y)_{i+1} \cos \alpha \quad (\text{tension}) \quad (8b)$$

Furthermore, a vertical force  $P_{\text{unb}}$  because of the BRB's axial strength greater in compression than in tension produces shear force and bending moment on the beams

$$P_{\text{unb},i} = (\beta \omega N_y - \omega N_y)_i \sin \alpha \quad (9)$$

Finally, the axial force of the column at the  $i$ -th story is evaluated by the vertical equilibrium of the columns above the story under examination (Figure 3(c))

$$N_{\text{Ed},i}^{\text{c}} = \sum_{k=i+1}^N \left[ (\beta \omega N_y)_k \sin \alpha - \frac{P_{\text{unb},k}}{2} + P_k \right] \quad (10)$$

where  $P_k$  is the gravity load acting on the column of the  $k$ -th story in the seismic design situation and  $N$  is the number of stories.

### 3.3. $P$ - $\Delta$ effects

$P$ - $\Delta$  effects are considered in the design procedure. In particular, the sensitivity parameter  $\theta$  is calculated at each story by the following equation:

$$\theta_i = \frac{q}{V_{\text{Ed},i} h} \sum_{j=i}^N \Delta u_j P_j \quad (11)$$

where  $V_{\text{Ed},i}$  is the design story shear,  $\Delta u_i$  is the story drift provided by the design seismic forces and  $P_j$  is the gravity load in the seismic design situation of the  $j$ -th story. Then, as stipulated by EC8,  $P$ - $\Delta$  effects are neglected if the maximum value of  $\theta_i$  is lower than 0.1, while these effects are considered by amplifying the design axial forces in braces by the coefficient  $1/(1 - \theta_i)$  if the maximum value of  $\theta_i$  is higher than 0.1 and lower than 0.2. No value of  $\theta_i$  higher than 0.3 is accepted.

## 4. ANALYZED BUILDINGS

The design procedure is applied to 4-story, 8-story, and 12-story buildings standing on soft soil. The BRBs in the chevron configuration are located in the central span of the frames on the perimeter of the building (Figure 4). All beam-to-column connections are assumed to be pinned, and the whole seismic force is sustained by the chevron braces. The columns belonging to the braced frames (CB) are oriented with their strong axis orthogonal to the plane of the braced frame. The columns devoted to sustain gravity loads (hereinafter named gravity columns), instead, are indicated by the symbols CL and CC and are oriented with their strong axis orthogonal to the  $Y$ -direction and  $X$ -direction, respectively.

The total seismic force is evaluated by the elastic spectrum proposed by EC8 for soil type C, characterized by a peak ground acceleration  $a_g$  equal to  $0.35g$ , and reduced by the behavior factor  $q$ . Each frame is designed by means of several values of  $q$  ranging from 2.5 (which is the value stipulated by EC8 for conventional chevron braced frames) to 6.5 in steps of 1.0.

Story mass is estimated according to EC8 by taking into account the dead and live load of  $5.0 \text{ kN/m}^2$  present in the building on the occurrence of the earthquake and evaluated as shown in Figure 4.

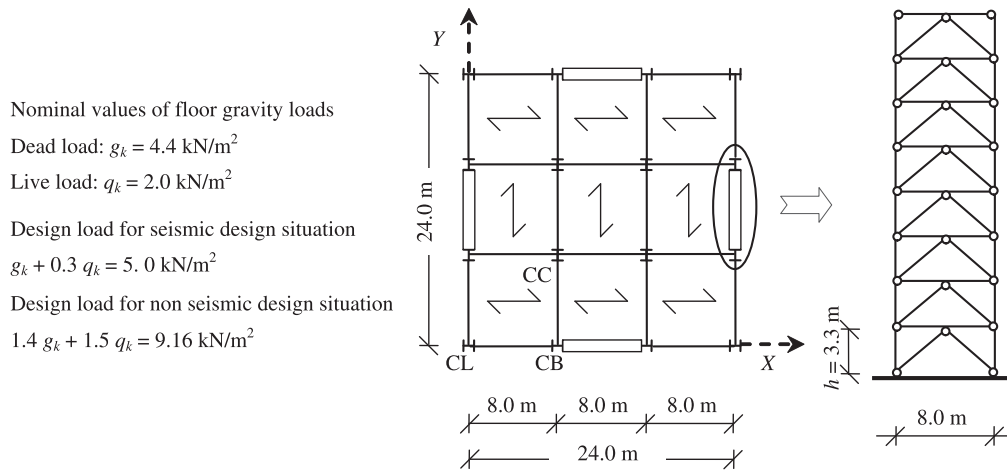


Figure 4. Layout of the analyzed frames.

Frames are designed by means of three values of the design story drift  $\Delta u^d$  to consider different levels of available ductility of BRBs. Specifically, the story drift angle  $\Delta^d$ , that is, the ratio of the design story drift to the interstory height, is fixed equal either to 1.0%, 1.5% or 2.0%.

Steel grade S 235 ( $f_y = 235 \text{ MPa}$ ) is used for all the braces. In accordance with common application of BRBs, the length of the yielding core is supposed to be equal to  $0.5 L_w$ . The restrained and unrestrained nonyielding segments are characterized by  $A_c/A_t = 0.5$  and  $A_c/A_j = 0.3$  [31]. The lengths of each part of the unrestrained nonyielding segment and of the restrained yielding segment are  $L_j / 2 = 0.65 \text{ m}$  and  $L_t / 2 = 0.5 (L_w - L_c - L_j)$ .

The internal forces of beams and columns are determined according to the procedure described in Section 3.2. The compression strength adjustment factor  $\beta$  is assumed to be unitary while the tension strength adjustment factor  $\omega$  is calculated at each story as a function of the available ductility  $\mu_{\max}$  and of the post-yield stiffness ratio  $k_h$  by the following equation:

$$\omega_i = 1 + k_h \cdot (\mu_{\max,i} - 1) \quad (12)$$

Beam and column cross-sections are selected among the European wide flange shapes (HEA for the beams, HEB or HEM for the columns) so that the design axial force is lower than the buckling resistance determined according to EuroCode 3 (EC3) [32]. The partial safety coefficient  $\gamma_{M1}$  is assumed equal to 1. Rarely, some column sections of the lower stories are obtained from two IPE shapes welded to the web of a HEB or HEM shape to obtain similar moments of inertia with respect to the principal axes of the cross-section. Steel grade S 235 is used for all the beams; steel grade S 235, S 275 ( $f_y = 275 \text{ MPa}$ ) or S 355 ( $f_y = 355 \text{ MPa}$ ) is used for the columns. According to conventional design practice, the same column cross-section is adopted for two consecutive stories.

The gravity columns are designed considering the load per square meter for nonseismic design situation, which is equal to  $9.16 \text{ kN/m}^2$  (Figure 4). Because all beam-to-column connections are pinned, no bending moment is induced in the column by vertical loads; the axial force of the column is evaluated according to the tributary area concept. The required cross-section is determined by equating the buckling axial strength in the weak axis plane of the cross-section determined by EC3 [32] to the demanded axial force.

In the design of each considered structure,  $P-\Delta$  effects have been neglected at first. As an exemplary case, the maximum values of the stability coefficient factor for 8-story frames designed assuming different values of the behavior factor and a design story drift angle equal to 1.5% are listed in Table I. Note that for the 8-story frames with  $\Delta^d = 1.5\%$ , systems designed with  $q$  equal to 4.5, 5.5, and 6.5 are characterized by values of  $\theta_{\max}$  larger than 0.1. For this reason, the design of these three frames (and of all the other frames with  $\theta_{\max} > 0.1$ ) has been repeated taking into account the  $P-\Delta$  effects according to the provision of the EC8.

Table I. Maximum coefficient of sensitivity to  $P$ - $\Delta$  effect for 8-story frames,  $\Delta^d = 1.5\%$ .

$q = 2.5$	$q = 3.5$	$q = 4.5$	$q = 5.5$	$q = 6.5$	$q = 4.5^*$	$q = 5.5^*$	$q = 6.5^*$
0.031	0.066	0.130	0.194	0.194	0.103	0.162	0.176

\*designed taking into account the  $P$ - $\Delta$  effects

#### 4.1. Influence of the behavior factor on the designed structures

The reduction of the design seismic forces because of high values of  $q$  leads to small values of the area of the cross-section adopted for BRBs. Consequently, the higher the value of the behavior factor, the greater the period of the designed frames. This aspect is underlined in Figure 5(a) with reference to 4-story systems designed without  $P$ - $\Delta$  effects. This figure shows the elastic and the design response spectra obtained with reference to three different values of the behavior factor (2.5, 4.5, and 6.5) and the periods  $T_1$  of the first mode of vibration of the 4-story frames designed by these values of  $q$ . However, very high values of the design behavior factor are sometimes fictitious, because they do not cause a reduction of the seismic design forces because of the design spectrum shape. Indeed, the design pseudo-acceleration obtained by an assigned value of the behavior factor cannot be lower than  $S_{a,\min} = 0.2 a_g$  [1]; the symbol  $T^{*(q)}$  is adopted in Figure 5(a) to represent the smallest period of vibration for which the design value of pseudo-acceleration is equal to  $S_{a,\min}$ . Note that the value of  $T^{*(q)}$  decreases with  $q$ . The reduction of the seismic design forces of the first mode of vibration because of an increase in the adopted value of  $q$  is null with reference to systems for which  $T^{*(q)}$  is lower than  $T_1$ . Hence, the core of BRBs of 4-story systems designed by two contiguous values of  $q$  change significantly because these systems have fundamental periods of vibration lower than  $T^{*(q)}$  unless a very high value of the design behavior factor is adopted. Instead, the core of BRBs of 12-story systems (which have high values of  $T_1$ ) designed by two contiguous values of  $q$  is almost the same even when rather low values of  $q$  are adopted. This aspect is remarked in Figure 5(b). This figure shows that the pseudo-accelerations corresponding to the fundamental periods of the 12-story structures designed by  $q$  equal to 4.5 and 6.5 are exactly the same. The small difference in the period of vibration of these structures is due to the reduction of the seismic forces of higher modes of vibration when a value of  $q$  equal to 6.5 is adopted.

These considerations are confirmed by Figure 6 in which the periods of the first mode of vibration of all the designed structures are plotted as a function of the behavior factor. Frames with 4, 8, or 12 stories are represented by different symbols. A different color, grey or white, is used to differentiate between systems designed taking into account  $P$ - $\Delta$  effects or not, respectively. When  $P$ - $\Delta$  effects are taken into account (grey symbols in the figure) the area of the cross-sections required by the design seismic forces is increased as a function of the story stability coefficient factor  $\theta_i$ . As the values of  $\theta_i$  and of the amplification factor  $1/(1 - \theta_i)$  increase with the behavior factor, the reduction of the adopted area because of the increase of  $q$  is less remarkable in structures designed taking into account  $P$ - $\Delta$  effects rather than in structures designed neglecting  $P$ - $\Delta$  effects.

On the basis of the previous considerations, first the mean value along the height of the cross-section area of the BRB's yielding core  $\bar{A}_c$  is calculated for each structure obtained for  $q$  in the range 2.5–6.5 in

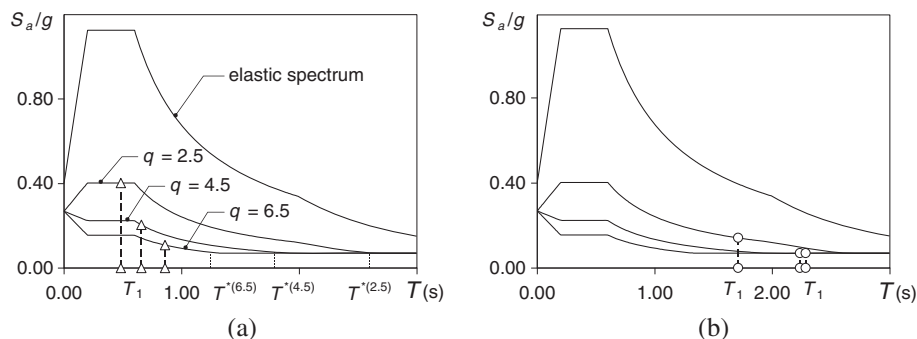


Figure 5. Design spectra and periods of (a) 4-story frames and (b) 12-story frames.

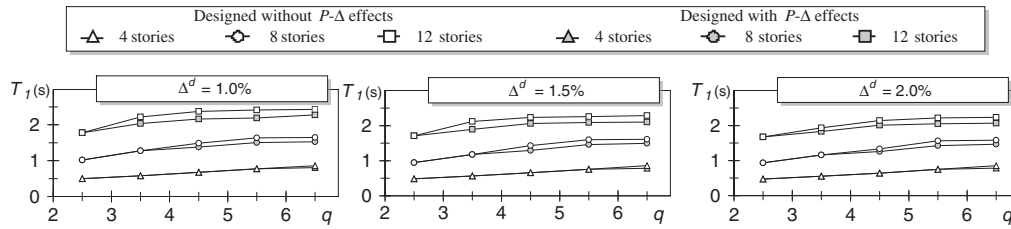


Figure 6. Periods of the first mode of vibration of the designed frames.

steps of 1 (see, as an example, Table II with reference to 8-story frames designed assuming  $\Delta^d$  equal to 1.5% and neglecting  $P$ - $\Delta$  effects). Second, the percentage reduction of  $\bar{A}_c$  because of the adoption of a higher value of the behavior factor is estimated as

$$\Delta \bar{A}_c(\%) = \frac{\bar{A}_c(q) - \bar{A}_c(q-1)}{\bar{A}_c(q-1)} \quad (13)$$

Finally, the value of the behavior factor  $q^{up}$ , which corresponds to a prefixed percentage reduction of  $\bar{A}_c$  is calculated by linear interpolation. In particular, a percentage reduction equal to 15% is fixed (as an example see the obtained values of  $q^{up}$  in Tables III and IV), because by doing so frames designed by means of  $q$  higher than  $q^{up}$  are almost coincident to those obtained when a behavior factor equal to  $q^{up}$  is considered. As an example, when  $\Delta^d$  is equal to 1.5% the value of  $q^{up}$  is equal to 4.45 and 5.92 (see Table III) for 12-story and 8-story frames designed neglecting  $P$ - $\Delta$  effects, respectively. The periods of the frames designed by these values of  $q$  are 2.23 and 1.60 s (see Figure 6) and they are virtually the same for larger values of  $q$ .

Table II. Cross-sectional area of the yielding core of BRB for 8-story frames,  $\Delta^d = 1.5\%$  and  $P$ - $\Delta$  effects neglected.

Story	$q=2.5$	$q=3.5$	$q=4.5$	$q=5.5$	$q=6.5$
Cross-sectional area (cm <sup>2</sup> ) of the yielding core					
8	18.45	11.49	8.07	6.29	5.75
7	30.24	18.29	12.47	9.62	9.04
6	38.99	22.97	15.20	11.61	11.23
5	46.06	26.73	17.30	13.09	12.95
4	52.17	30.19	19.47	14.68	14.60
3	57.41	33.50	21.79	16.47	16.25
2	61.55	36.32	23.95	18.21	17.73
1	63.92	38.04	25.35	19.36	18.67
Mean value of $A_c$ (cm <sup>2</sup> ) of the yielding core					
$\bar{A}_c$	46.10	27.19	17.95	13.67	13.28

Table III. Reduction of the mean value of  $\bar{A}_c$  because of the adoption of higher value of  $q$ ,  $\Delta^d = 1.5\%$  and  $P$ - $\Delta$  effects neglected.

$q$	4-Story		8-Story		12-Story	
	$\bar{A}_c$ (cm <sup>2</sup> )	$\Delta \bar{A}_c(\%)$	$\bar{A}_c$ (cm <sup>2</sup> )	$\Delta \bar{A}_c(\%)$	$\bar{A}_c$ (cm <sup>2</sup> )	$\Delta \bar{A}_c(\%)$
2.5	39.96		46.10		40.69	
3.5	28.59	28%	27.19	41%	23.17	43%
4.5	20.40	29%	17.95	34%	19.80	15%
5.5	14.61	28%	13.67	24%	18.94	4%
6.5	11.01	25%	13.28	3%	18.41	3%
$q^{up}$	—		5.92		4.45	

Table IV. Reduction of the mean value of  $\bar{A}_c$  because of the adoption of higher value of  $q$ ,  $\Delta^d = 1.5\%$  and  $P$ - $\Delta$  effects taken into account.

$q$	4-Story		8-Story		12-Story	
	$\bar{A}_c$ (cm <sup>2</sup> )	$\Delta\bar{A}_c(\%)$	$\bar{A}_c$ (cm <sup>2</sup> )	$\Delta\bar{A}_c(\%)$	$\bar{A}_c$ (cm <sup>2</sup> )	$\Delta\bar{A}_c(\%)$
2.5	39.96		46.10		40.69	
3.5	28.59	28%	27.19	41%	29.68	27%
4.5	20.40	29%	21.61	21%	23.37	21%
5.5	14.61	28%	16.95	22%	22.29	5%
6.5	13.25	9%	15.82	7%	21.71	3%
$q^{up}$	6.20		5.94		4.87	

#### 4.2. Influence of the design story drift

The design story drift mainly affects the maximum ductility  $\mu_{max}$  that BRBs have to be able to sustain. In Table V, the distribution along the height of the required ductility in 8-story frames designed by means of a behavior factor equal to 4.5 and by different values of the design story drift angle is compared. The required ductility is generally greater at the lower stories but it is almost constant in elevation. Its mean value is equal to 10.9, 17.3, and 23.8 for systems characterized by a design story drift angle equal to 1.0%, 1.5%, and 2.0%, respectively. It is worth noting that the required ductility does not significantly change if referred to systems designed with the other considered values of the behavior factor.

According to Equation (12), the tension strength adjustment factor  $\omega$  of the BRBs at each story can be calculated as a function of the required ductility. Because beams and columns are designed according to the capacity design principles assuming that braces are fully yielded and hardened, the design seismic actions on these members are greater when higher values of the design story drift are considered. For this reason, the area of the cross-section required for beams and columns are generally greater for systems designed by  $\Delta^d$  equal to 2.0%. Despite this, the cross-sections adopted are not very different because of the limited number of wide flange commercial profiles adopted for these members. Note that, because of the considerations above, frames designed with higher values of the design story drift angle are generally stiffer than those designed with  $\Delta^d$  equal to 1.0%. The reduction of the fundamental period of vibration also leads to generally higher design seismic forces and consequently to a slight increase in the cross-sectional area required for braces.

#### 4.3. Verification of the damage limitation requirement

All the considered frames are designed with reference to the life safety performance level, the fulfillment of the damage limitation requirement is checked *a posteriori*. In particular, the serviceability limit state of the frames is checked according to the provisions stipulated in EC8 [1]. The story drift angle  $\Delta_r$  demanded by the moderate earthquake with a 10% probability of exceedance in 10 years is evaluated as

Table V. Required ductility for BRB of 8-story frames designed with  $q$  equal to 4.5,  $P$ - $\Delta$  effects neglected.

Story	$\Delta^d = 1.0\%$	$\Delta^d = 1.5\%$	$\Delta^d = 2.0\%$
8	10.48	16.85	23.41
7	10.35	16.72	23.30
6	10.37	16.75	23.39
5	10.56	17.02	23.64
4	10.82	17.26	23.84
3	11.27	17.68	24.13
2	11.57	17.95	24.38
1	11.94	18.29	24.61
Mean	10.92	17.31	23.84

$$\Delta_r = \frac{v \Delta u_e}{h} \quad (14)$$

where  $v$  is the reduction factor to take into account the lower magnitude of the moderate earthquake (set at 0.5 for ordinary buildings) and  $\Delta u_e$  is the elastic story drift provided by the unreduced seismic force. The story drift angle  $\Delta_r$  should be smaller than an assigned limit, which is fixed on the basis of the type of nonstructural elements present in the building. Specifically, it is equal to 0.50% or 0.75% if brittle or ductile nonstructural elements are used in the building, it is equal to 1.00% if nonstructural elements do not interfere with structural deformations.

In Figure 7 the maximum story drift angle is plotted as a function of the behavior factor adopted. All the designed structures fulfill the damage limitation requirements if nonstructural elements do not interfere with structural deformations (1%) while only 4-story frames satisfy the limit on the maximum story drift angle of 0.50%.

## 5. NONLINEAR DYNAMIC ANALYSES

The seismic response of all the designed frames is evaluated by nonlinear dynamic analysis carried out by means of the OpenSees computer program [33]. A Rayleigh viscous damping is used and set at 3% for the first and the second modes of vibration. The  $P$ - $\Delta$  effects are included in the analysis. The suite of 20 ground motions [34] adopted in the FEMA/SAC project, representing seismic events having a 10% probability of exceedance in 50 years in the US Los Angeles area, is used in this study. All the accelerograms are scaled by a factor 0.88 so that the mean 5% damped spectrum of the 20 ground motions matches the EC8 spectrum used in design as shown in Figure 8. The results of nonlinear dynamic analysis are used to evaluate the seismic demand expressed in terms of ductility of BRBs and internal forces of nondissipative members (beam and columns of the braced frame, gravity columns). Then, the seismic demand is compared with the capacity of the designed structures to select the highest value of  $q$ , which leads to the achievement of the life safety limit state.

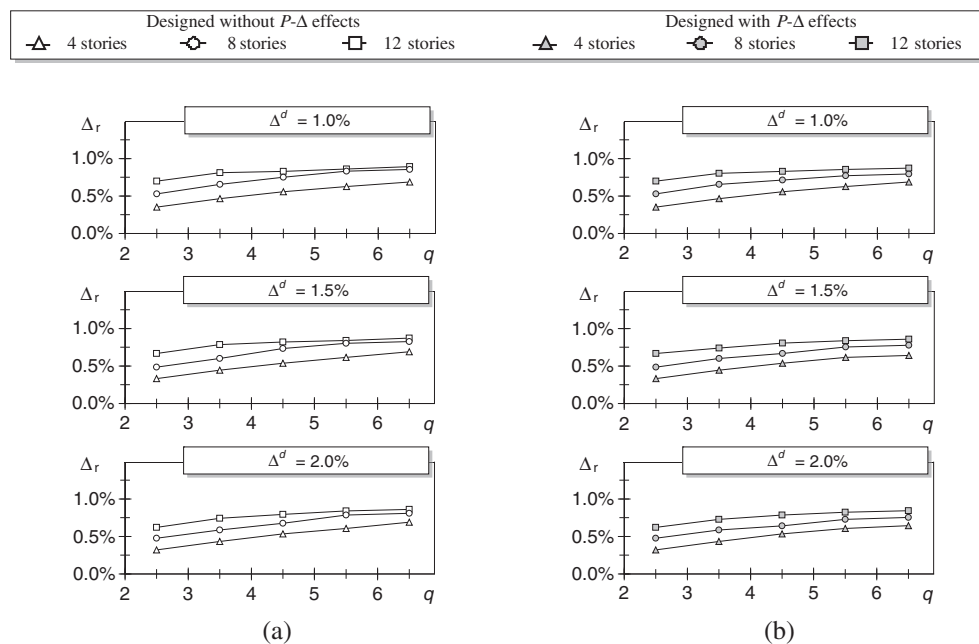


Figure 7. Maximum story drift angle for the damage limitation limit state: systems designed (a) neglecting or (b) taking into account  $P$ - $\Delta$  effects.

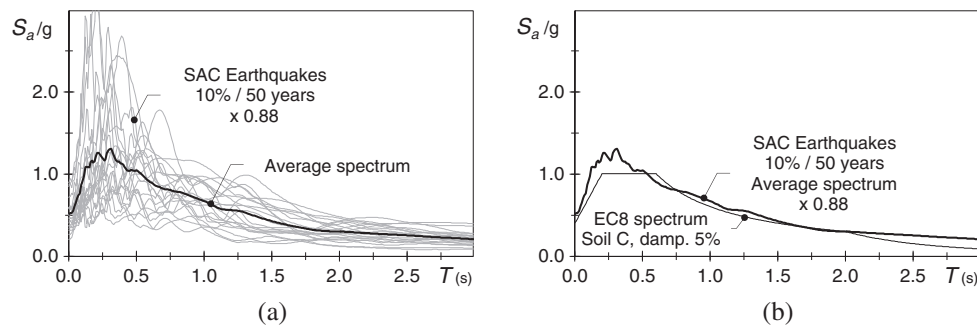


Figure 8. Response spectra: (a) individual adopted ground motions and (b) comparison between the EC8 spectrum and the average spectrum.

### 5.1. Numerical model

Because of the symmetry of the spatial structure, the numerical analyses are carried out on a two-dimensional model that represents half the structure of the building. Thus, the structural model analyzed in this section include the frame with BRBs and six columns, which are pinned at the base (Figure 9): two gravity columns oriented to provide the maximum lateral stiffness (CC-type columns), two gravity columns oriented to provide the minimum lateral stiffness (CL-type columns) and two columns belonging to the braced frame in the orthogonal direction (CB-type columns). Prior researches have demonstrated that the presence of continuous columns can reduce maximum and residual drift demands [5, 6] and promote a more uniform distribution of drift demand along the height of the building [35, 36]. This beneficial impact is counterbalanced by an increase in bending moments on the columns [36]. In the paper, the effect of gravity columns is taken into account considering two different configurations: indeed, the columns are supposed to be continuous either for the whole height of the building or for two consecutive stories (see Figure 9). The first configuration is more penalizing for columns while the second is more penalizing for BRBs. These two configurations will be hereinafter referred to as continuous columns or noncontinuous columns. The tributary gravity load is applied to each column of the numerical model.

Buckling restrained braces are modeled by means of three elements. The outermost elements are elastic and schematize the restrained and unrestrained nonyielding segments connected in series. Each of them is characterized by a length and a cross-sectional area equal to

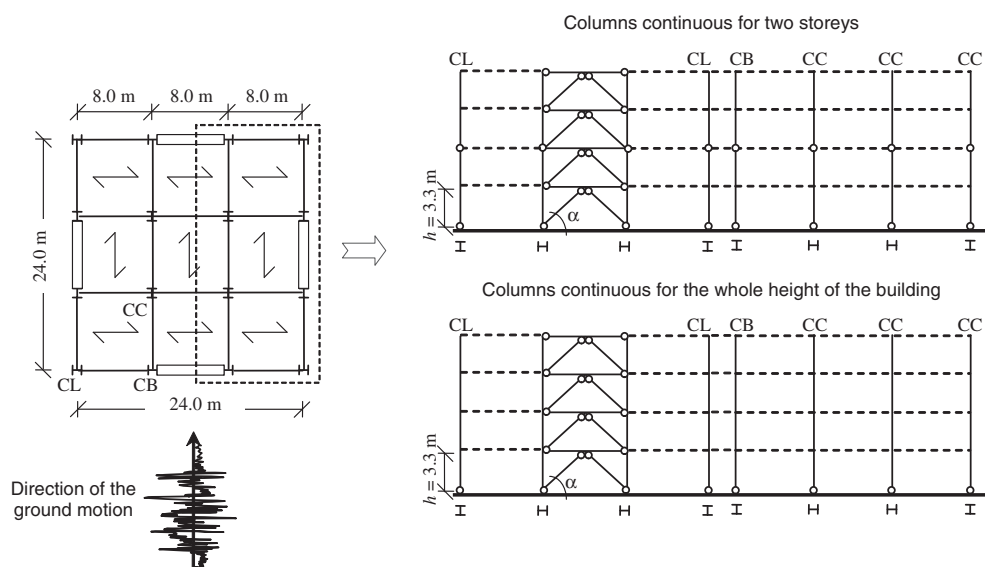


Figure 9. Numerical model of the frames.

$$L^1 = L^3 = \frac{L_j + L_t}{2} \quad (15)$$

$$A_i^1 = A_i^3 = \frac{A_{c,i}(L_j + L_t)}{L_j \frac{A_c}{A_j} + L_t \frac{A_c}{A_t}} \quad (16)$$

The central element simulates the yielding core. It is modeled by a ‘nonlinear BeamColumnElement’ with the cross-section defined by the ‘SectionAggregator object’ [33]. This command aggregates groups of uniaxial material objects into a single section model. In particular, an elastic behavior is considered with reference to flexure, while a uniaxial Giuffré–Menegotto–Pinto material object, which provides a good approximation of the actual smooth elastic–plastic transition, is defined to represent the section force–deformation response for the axial degree-of-freedom. This material object is characterized by a resistance equal to  $A_c f_y$ , a stiffness equal to  $EA_c$  and a strain-hardening ratio  $k_h^c$  (ratio between post-yield stiffness and initial elastic stiffness). The value of the strain-hardening ratio of the core  $k_h^c$  is calibrated so that the post-yield stiffness ratio of the whole BRB is equal to  $k_h$  (as defined in Section 2)

$$k_h^c = \frac{k_h}{1 + (1 - k_h) \left[ \frac{L_t A_c}{L_c A_t} + \frac{L_j A_c}{L_c A_j} \right]} \quad (17)$$

In particular, with reference to the values fixed for the ratios  $L_t/L_c$ ,  $L_j/L_c$ ,  $A_c/A_t$ ,  $A_c/A_j$ , the strain-hardening ratio of the yielding core is 3.88%.

Beams and columns of the braced frames are modeled by elastic beam–column elements.

## 5.2. Acceptance criteria

Several response parameters are calculated and used to compare the seismic response of the designed structures. For each nonlinear dynamic analysis, the maximum required ductility of braces is determined as the ratio of the maximum required axial elongation/shortening to the axial elongation at yielding

$$\mu_{\text{req}} = \frac{\max(\delta^+, -\delta^-) - \delta_y}{\delta_y} \quad (18)$$

The required axial elongation ( $\delta^+$ ) and shortening ( $\delta^-$ ) are due to the elastic and plastic deformation of the core and to the elastic deformation of the restrained and unrestrained nonyielding segments; the axial elongation of the brace at yielding is calculated as

$$\delta_y = \frac{f_y}{E} \left( L_j \frac{A_c}{A_j} + L_t \frac{A_c}{A_t} + L_c \right) \quad (19)$$

The required ductility is compared with a reference value of ductility. Since the EC8 does not provide specific provisions for BRBs, the reference value of ductility is assumed in analogy to what is stipulated by EC8 - part 3 [37] for the plastic rotation capacity of members in flexure. For these members the EC8 stipulates that the plastic rotation required by seismic events with a 10% probability of exceedance in 50 years (Life Safety limit state) has to be not larger than 3/4 of the ultimate plastic rotation. Therefore, in the paper the reference value of ductility is assumed equal to 3/4 of the ductility capacity  $\mu_{\text{max}}$  (as evaluated in Section 3.1). Values of the maximum normalized ductility demand  $\bar{\mu} = \mu_{\text{req}}/(3/4 \mu_{\text{max}})$  less or greater than 1 indicate whether the brace ductility required by the earthquake is less or greater

than that available, respectively. The BRB cumulative ductility demand, instead, is not considered in this investigation because typically it does not exceed the capacity [20].

Beams and columns of the braced frames and gravity columns are nondissipative members. Thus, inelastic deformations or buckling phenomena are not allowed. Hence seismic performance of the analyzed braced frames is also examined in terms of two maximum normalized resistance demands: the normalized axial force resistance demand  $\bar{N}$  and bending moment resistance demand  $\bar{M}$ . These response parameters are calculated as

$$\bar{N} = \max \left\{ \frac{N_{Ed}(t)}{N_{M,b,Rd}(t)} \right\}; \quad \bar{M} = \max \left\{ \frac{M_{Ed}(t)}{M_{N,Rd}(t)} \right\} \quad (20)$$

where  $M_{N,Rd}(t)$  is the design plastic moment resistance reduced because of the axial force  $N_{Ed}(t)$  at the time  $t$  and  $N_{M,b,Rd}(t)$  is the buckling resistance reduced because of the bending moment  $M_{Ed}(t)$ . Both flexural and buckling resistances are determined according to EC3 [32]. It is worth noting that the buckling resistance of the beam is calculated assuming that the out-of-plane buckling is restrained by the deck.

The maximum normalized resistance demands  $\bar{N}$  and  $\bar{M}$  are also assumed as indexes of the seismic performance. Beams and columns fulfill the life safety limit state requirement if the above mentioned ratios are lower than 1.0.

### 5.3. Seismic response of the designed structures

Figure 10 shows the distribution along the height of the normalized ductility demand of the braces of the 8-story frames designed by  $\Delta^d$  equal to 1.5%. The suite ground motions adopted in this study includes seismic events characterized by very scattered spectra (Figure 8(a)). Consequently, the seismic response, expressed in terms of normalized ductility demand, presents a significant extent of variation. Here, the value at each story is the median obtained for the 20 ground motions.

In particular, results refer to structures with noncontinuous columns. Each curve represents a frame designed by means of a different value of the behavior factor. Frames with noncontinuous columns and designed neglecting  $P$ - $\Delta$  effects have a normalized ductility demand lower than 1 at each story whether values of  $q$  up to 4.5 are adopted. Instead, the normalized ductility demand is greater than 1.0 at the two lower stories of frames designed by values of  $q$  equal to 5.5 and 6.5; thus these systems do not fulfill the life safety requirements. The continuity of the columns for the whole height of the building (Figure 10(b)) reduces the required normalized ductility at the lower stories and makes more

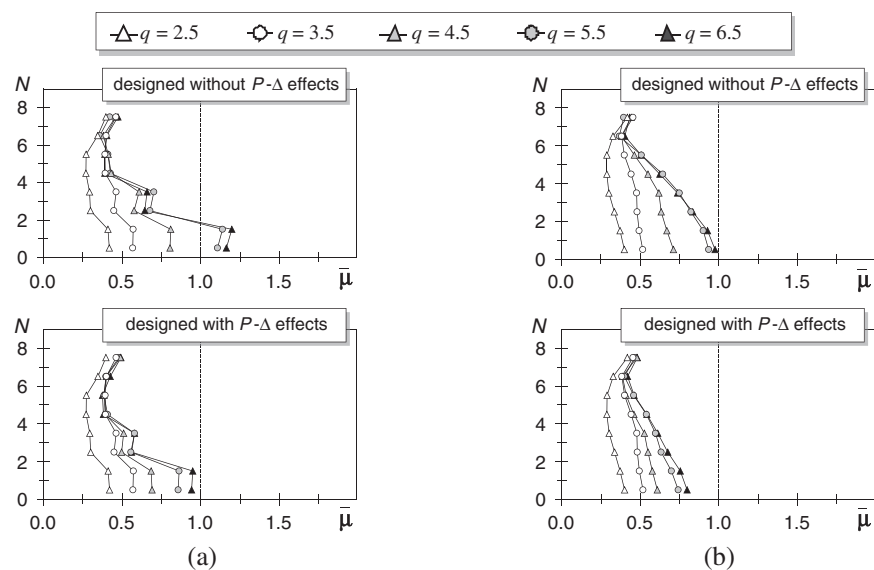


Figure 10. Normalized required ductility in braces for 8-story frames designed with  $\Delta^d = 1.5\%$ : (a) noncontinuous columns and (b) continuous columns.

uniform its distribution in elevation. Indeed, when continuous columns are adopted, a design behavior factor up to 6.5 can be adopted. When the structures are designed taking  $P-\Delta$  effects into account (Figures 10(a) and (b)), the values of the required normalized ductility are lower and all the 8-story frames designed by  $\Delta^d = 1.5\%$  are characterized by  $\bar{\mu} \leq 1$ .

The maximum normalized axial forces and bending moments for the columns belonging to the braced frame and for the gravity columns arranged to provide the maximum lateral stiffness (CC-type columns) are plotted in Figures 11 and 12 with reference to the previously mentioned 8-story frames designed by neglecting  $P-\Delta$  effects. Also in these cases the value at each story is the median obtained for the 20 ground motions. When the columns are continuous the normalized axial force  $\bar{N}$  and bending moment  $\bar{M}$  become greater. Nonetheless, all the nondissipative members are generally characterized by maximum values of the normalized axial force and bending moment lower than

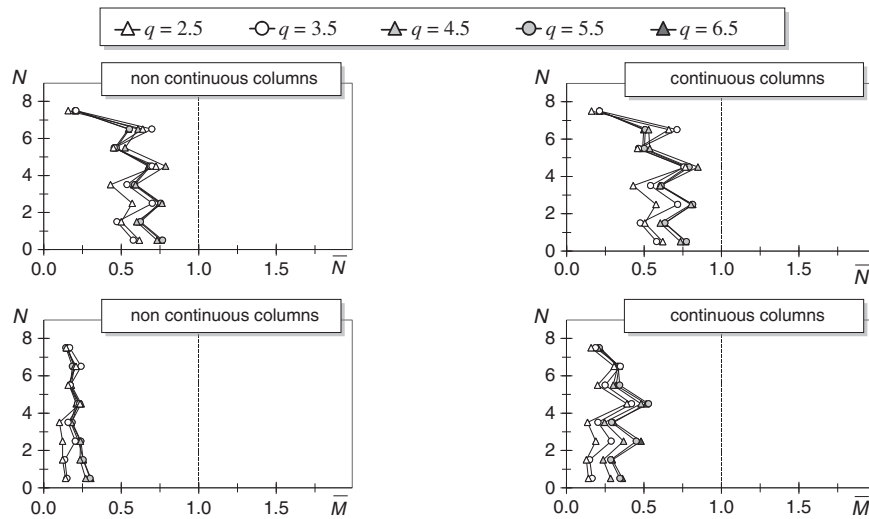


Figure 11. Normalized axial force and bending moment of columns of the braced frames for 8-story frames designed with  $\Delta^d = 1.5\%$  and without  $P-\Delta$  effects.

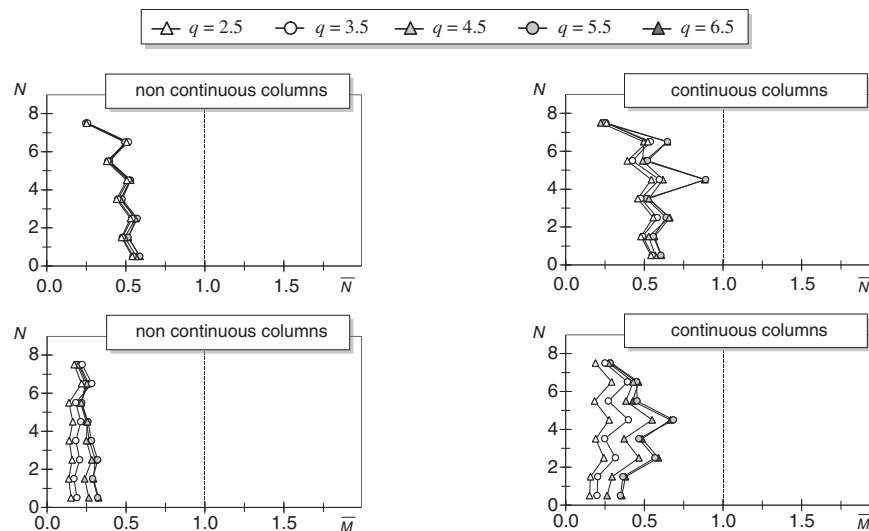


Figure 12. Normalized axial force and bending moment of CC-type gravity columns for 8-story frames designed with  $\Delta^d = 1.5\%$  and without  $P-\Delta$  effects.

1.0 at all the stories. Indeed, no yielding of nondissipative members occurs. In exceptional cases, buckling of gravity columns of some systems designed by the highest values of  $q$  may occur (not shown in figure). The buckling of the beams occurs only in a few cases (8-story frames designed with  $q$  equal to 5.5 and  $\Delta^d$  equal to 1.0%).

## 6. CALIBRATION OF THE BEHAVIOR FACTOR

One of the objectives of this study is to evaluate the maximum value of the behavior factor ( $q_{\max}$ ) that can be adopted for the design of braced frames endowed with BRBs. The value  $q_{\max}$  is determined for systems characterized by each considered design story drift angle, that is, systems characterized by different available ductility. Furthermore,  $q_{\max}$  is calibrated independently for systems designed whether taking into account  $P$ - $\Delta$  effects or not and modeled considering continuous or noncontinuous columns. Here, as an example, the procedure followed to evaluate the maximum value of  $q$  is described only for systems with noncontinuous columns and designed by  $\Delta^d = 1.5\%$ .

The maximum value along the height of the normalized ductility demand is calculated and plotted in Figure 13 as a function of the corresponding value of  $q$  for systems with 4, 8, and 12 stories. For systems designed by neglecting  $P$ - $\Delta$  effects (Figure 13(a)), it is possible to evaluate the value of  $q$  corresponding to  $\bar{\mu}_{\max} = 1$  by linear interpolation. It is worth noting that some of the systems designed by taking  $P$ - $\Delta$  effects into account (Figure 13(b)), are characterized by values of  $\bar{\mu}_{\max}$

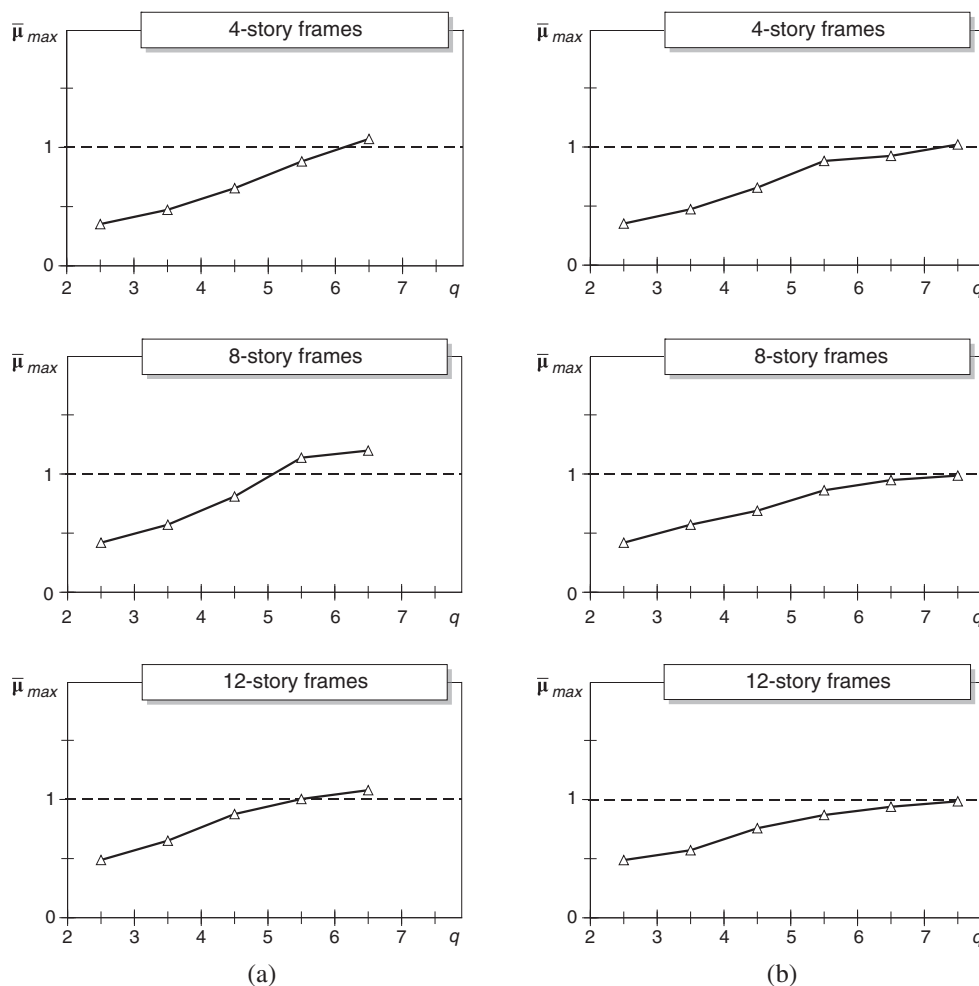


Figure 13. Evaluation of the behavior factor corresponding to  $\bar{\mu}_{\max} = 1$  in braces of systems (noncontinuous columns,  $\Delta^d = 1.5\%$ ) designed (a) without or (b) with  $P$ - $\Delta$  effects.

lower than 1 for all the considered behavior factors. In these cases, new frames have been designed by enlarging the range of the considered behavior factors.

The maximum values along the height ( $\bar{N}_{\max}$ ,  $\bar{M}_{\max}$ ) of the normalized axial force and bending moment strength demands are calculated for nondissipative members (Figure 14). The normalized axial force and bending moment of beams, columns of the braced frames (columns of BRBFs) and gravity columns (CC-type, CL-type, and CB-type columns) are represented by curves marked with different symbols. Figure 14 shows that the ratios  $\bar{M}_{\max}$  and  $\bar{N}_{\max}$  always remain smaller than unity. For systems with continuous columns (not shown in figure) the strength demand increases and the above mentioned ratios become larger than unity in a few cases for type CC gravity columns. In these cases, the values of  $q$  corresponding to  $\bar{M}_{\max} = 1$  or  $\bar{N}_{\max} = 1$  are calculated by linear interpolation.

At the end of this stage, the maximum value of the behavior factor  $q_{\max}$  that can be adopted to attain the available ductility of the braces ( $\bar{\mu}_{\max} = 1$ ) without buckling or yielding of nondissipative members is known.

In Figure 15(a)  $q_{\max}$  is plotted as a function of the design story drift angle for systems with noncontinuous columns designed by neglecting  $P$ - $\Delta$  effects. Again different symbols are adopted to pinpoint systems with a different number of stories. When the design assumptions lead to systems characterized by  $\bar{\mu}_{\max}$ ,  $\bar{M}_{\max}$ ,  $\bar{N}_{\max} < 1$  independently of the assumed behavior factor, the values  $q^{\text{up}}$  determined in Section 4.1 are reported in the figure instead of  $q_{\max}$ . Furthermore, the corresponding symbols are coupled with an up arrow to underline that values of  $q$  higher than  $q^{\text{up}}$  can also be adopted because they lead to frames virtually identical to that obtained by  $q^{\text{up}}$ . The condition  $\bar{\mu}_{\max}$ ,  $\bar{M}_{\max}$ ,  $\bar{N}_{\max} < 1$  generally occurs when medium or high rise structures characterized by a remarkable available ductility ( $\Delta^d = 2.0\%$ ) are considered. The same considerations

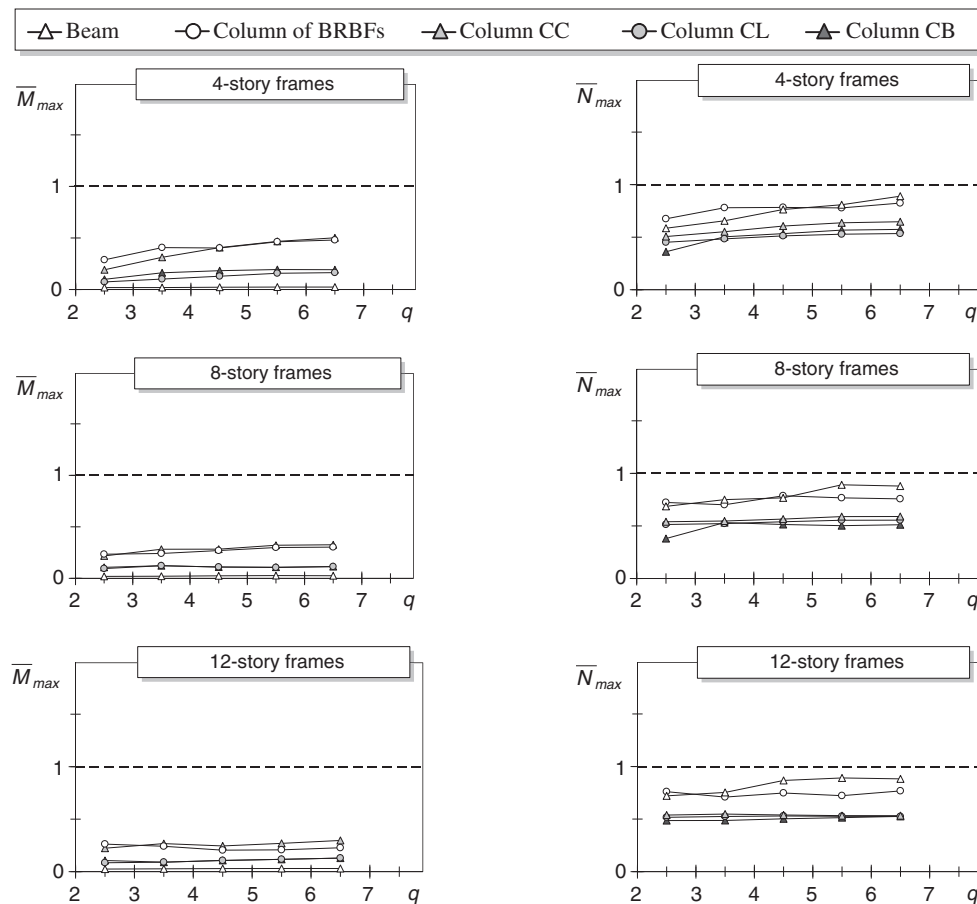


Figure 14. Evaluation of the behavior factor corresponding to the yielding or buckling of nonductile members (noncontinuous columns,  $\Delta^d = 1.5\%$ ,  $P$ - $\Delta$  effects neglected).

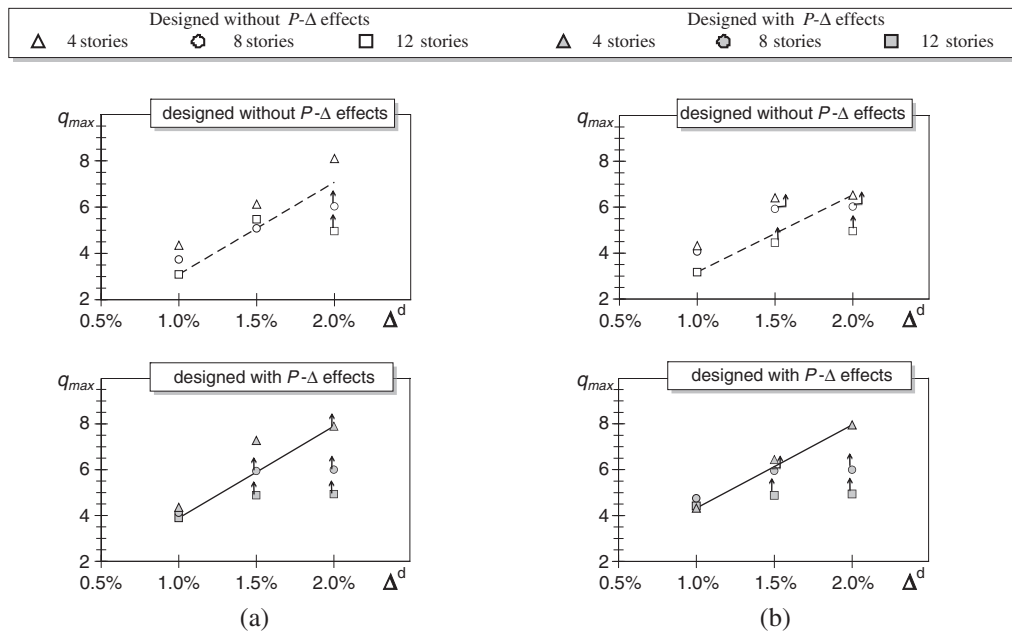


Figure 15. Calibration of the behavior factor for systems with: (a) noncontinuous columns and (b) continuous columns.

apply to systems with continuous columns designed by taking into account  $P$ - $\Delta$  effects (Figure 15). Note that the obtained values of the behavior factor generally decrease as the height of the building increases. This finding is consistent with the results of other studies concerning the evaluation of the response modification factor of frames endowed with BRBs [11–13] or other braced frames [36, 38–40]. However the values of  $q$  here obtained are significantly lower than those reported in [11–13] especially in regard to 4-story frames.

Analytical equations are here calibrated to select a proper value of the behavior factor as a function of the design story drift. In particular, the linear equations reported in Table VI are proposed. The values  $q_{\max}$  obtained by the equations are superimposed to those evaluated by the numerical analyses. Note that all the points representative of the behavior factors obtained by numerical analysis are close to the suggested values. Indeed, the values provided by the proposed equations generally fit the values of the behavior factor determined by numerical analysis well although sometimes they can lead to conservative values for low rise structures.

## 7. VALIDATION OF THE PROPOSED BEHAVIOR FACTOR

To validate the proposed behavior factor with reference to systems that are different from those adopted for its calibration, 4-story, 8-story, and 12-story frames with BRBs designed with  $\Delta^d$  either equal to 1.25% or 1.75% are analyzed. These systems are designed either by neglecting or taking into account  $P$ - $\Delta$  effects and assuming that columns are continuous for the whole height of the building or for two consecutive stories. According to the proposed formulae, the values of the behavior factor listed in Table VII are assumed.

Table VI. Proposed behavior factors for  $\Delta^d \leq 2.0\%$ .

Type of column	Designed without $P$ - $\Delta$ effects	Designed with $P$ - $\Delta$ effects
Continuous columns	$q_{\max} = 335 \Delta^d (\%) - 0.2$	$q_{\max} = 360 \Delta^d (\%) + 0.7$
Noncontinuous columns	$q_{\max} = 400 \Delta^d (\%) - 1.0$	$q_{\max} = 400 \Delta^d (\%) - 0.1$

Table VII. Behaviour factors adopted.

Type of column	Designed without $P$ - $\Delta$ effects		Designed with $P$ - $\Delta$ effects	
	$\Delta^d = 1.25\%$	$\Delta^d = 1.75\%$	$\Delta^d = 1.25\%$	$\Delta^d = 1.75\%$
Continuous columns	$q_{\max} = 4.0$	$q_{\max} = 5.7$	$q_{\max} = 5.2$	$q_{\max} = 7.0$
Noncontinuous columns	$q_{\max} = 4.0$	$q_{\max} = 6.0$	$q_{\max} = 4.9$	$q_{\max} = 6.9$

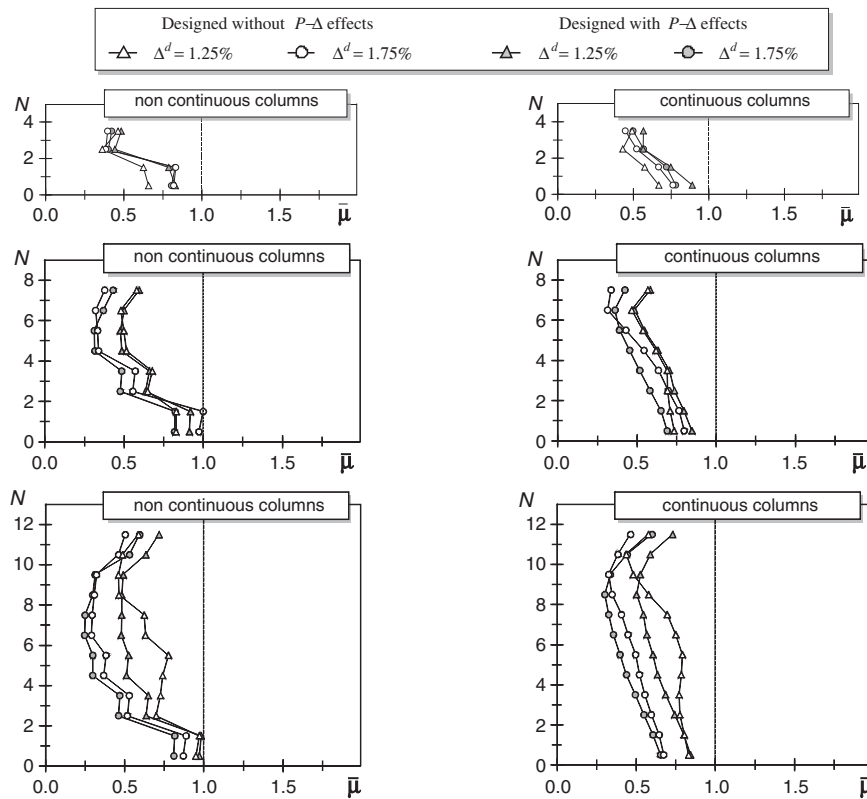


Figure 16. Normalized ductility demand of braces in systems designed according to the proposed values of the behavior factor.

The seismic response of the designed frames is evaluated by nonlinear dynamic analysis and represented in Figure 16 in terms of normalized ductility demand  $\bar{\mu}$  of braces. All the designed frames are characterized by maximum values of  $\bar{\mu}$  lower than 1.0. With reference to systems with noncontinuous columns, the maximum values of the normalized ductility are always close to 1.0 especially for medium or high rise structures. On the basis of these results the adopted values of  $q_{\max}$  seem to be effective and do not lead to oversized structures.

The maximum values of the normalized ductility are lower than 1.0 with a wider margin for systems with continuous columns. In this case too, however, the structures are not over-dimensioned because, as underlined in Section 4.1, the adoption of higher values of  $q$  would not provide a remarkable reduction of the seismic force and thus of the cross-section of structural members.

The seismic response of the designed structures are also appreciable in terms of the maximum normalized axial force and bending moment of nondissipative members (not shown in any figure). Indeed, it has been found that the maximum values of the normalized axial force and bending moment demands are always lower than 1.0.

## 8. CONCLUSIONS

The paper presents a procedure for the seismic design of steel frames with pinned beam-to-column connections equipped with BRBs and proposes a proper value of the behavior factor  $q$  to be adopted. The proposed method is developed for EuroCode 8 primarily, but the design procedure can be adjusted and incorporated into other codes. According to this procedure, braces are designed to sustain seismic design force based on the elastic response spectrum reduced by the behavior factor  $q$ . Furthermore, the available ductility of braces is determined so that they can accommodate a prefixed design story drift. In compliance with the capacity design principle, beams and columns are designed to resist internal forces obtained by the equilibrium of the frame when all the braces are fully yielded and have attained the maximum ductility capacity.

On the basis of the seismic response of a large set of concentrically braced frames equipped with BRBs in the chevron configuration, it was found that the choice of the behavior factor  $q$  to adopt depends on the design story drift. The presence of continuous columns has beneficial effects on the seismic response of the frames and generally allows an increase in the value of  $q$ . Furthermore, the value of  $q$  that can be adopted if  $P$ - $\Delta$  effects are included in the design procedure is larger than that obtained if  $P$ - $\Delta$  effects are neglected.

The results of the numerical investigation are used to define linear equations that provide the proper value of the behavior factor as a function of the design story drift. Specifically, four equations are calibrated to evaluate the behavior factor. Each equation, which is valid for design story drift not larger than 2%, refers to systems designed either by considering  $P$ - $\Delta$  effects or not doing so in the case of columns which are continuous for the whole height of the building or for two stories only.

Finally, the effectiveness of the proposed equations has been verified by a set of frames different from those adopted in the calibration phase. The seismic response of these frames subjected to a set of ground motions representing seismic events having a 10% probability of exceedance in 50 years has been evaluated by nonlinear dynamic analysis. The results have demonstrated that the seismic demand, in term of ductility for BRBs and strength for nondissipative members, never exceeded the capacity.

## ACKNOWLEDGEMENTS

The Authors wish to thank eng. Rosario Adamo for his contribution to the numerical analyses performed in the context of his graduation thesis.

## REFERENCES

1. CEN. *Draft n. 6 of EuroCode 8: Design provisions for earthquake resistance – Part 1: General rules, seismic actions and rules for buildings*. European Committee for Standardization: Bruxelles, 2003.
2. Della Corte G, D'Aniello M, Landolfo R, Mazzolani FM. Review of steel buckling-restrained braces. *Steel Construction* 2011; 4(2):85–93.
3. Uang CM, Nakashima M. *Earthquake Engineering: From Engineering Seismology to Performance Based Engineering*. CRC Press LLC: New York, 2004.
4. Xie Q. State of the art of buckling-restrained braces. *Journal of Constructional Steel Research*, 2005; 61:727–748.
5. Ariyaratana C, Fahnstock LA. Evaluation of buckling-restrained braced frames seismic performance considering reserve strength. *Engineering Structures* 2011; 33:77–89.
6. Kiggins S, Uang CM. Reducing residual drift of buckling-restrained braced frames as a dual system. *Engineering Structures* 2006; 28:1525–1532.
7. SEAONC (Structural Engineers Association of Northern California). *Recommended provisions for buckling restrained braced frames*. SEAONC: San Francisco, 2001.
8. Sabelli R, Aiken I. Development of Building Code Provisions for Buckling-Restrained Braced Frames. *Behavior of steel structures in seismic areas, Proceedings of the 4<sup>th</sup> international conference STESSA 2003*, Mazzolani F (ed.). A. A. Balkema Publishers: Naples, Italy, 2003; 813–818.
9. FEMA 450. *NEHRP recommended provisions for seismic regulations for new buildings and other structures*. Federal Emergency Management Agency: Washington, D.C., USA, 2004.
10. AISC 2005. *Seismic Provision for structural steel buildings*. American Institute of Steel Construction: Chicago, 2005.
11. Asgarian B, Shokrgozar HR. BRBF response modification factor. *Journal of Constructional Steel Research* 2009; 65:290–298.

12. Mahmoudi M, Zaree M. Evaluating response modification factors of concentrically braced steel frames. *Journal of Constructional Steel Research* 2010; **66**:1196–1204.
13. Kim J, Park J, Kim S. Seismic behavior factors of buckling restrained braced frames. *Structural Engineering and Mechanics* 2009; **33**(3):261–284.
14. Sabelli R, Mahin SA, Chang C. Seismic demands on steel braced frame buildings with buckling-restrained braces. *Engineering Structures* 2003; **25**:655–666.
15. Fahnestock LA, Sauce R, Ricles JM. Seismic response and performance of buckling restrained braced frame. *Journal of Structural Engineering* 2007; **133**(9):1195–1204.
16. Fahnestock LA, Sauce R, Ricles JM. Experimental evaluation of a large-scale buckling-restrained braced frame. *Journal of Structural Engineering* 2007; **133**(9):1205–1214.
17. Castaldo C, Della Corte G, Mazzolani FM. Towards the behavior factor of steel frames with BRB braces. *Proceedings of the XXII CTA*, 2009; 185–194, (in Italian).
18. Marino EM, Ghersi A, Nakashima M. Behavior factor for steel frames with buckling restrained braces. *Proceedings of the XXI CTA*, 2007; 185–192.
19. Black CJ, Makris N, Aiken ID. Component Testing, Stability Analysis and Characterization of Buckling Restrained 'Unbonded' Braces. *Technical Report PEER 2002/08, Pacific Earthquake Engineering Research Center*, University of California, Berkeley, 2002.
20. Fahnestock LA, Sauce R, Ricles JM, Lu LW. Ductility demands on buckling-restrained braced frames under earthquake loading. *Earthquake Engineering and Engineering Vibration* 2003; **2**(2):255–268.
21. Iwata M, Kato T, Wada A. Performance evaluation of buckling restrained braces in damage-controlled structures. *Behavior of steel structures in seismic areas, Proceedings of the 4<sup>th</sup> international conference STESSA 2003*, Mazzolani F (ed.). A.A. Balkema Publishers: Naples, Italy, 2003; 37–43.
22. Iwata M, Kato T, Wada A. Buckling restrained braces as hysteretic dampers. *Behavior of steel structures in seismic areas, Proceedings of the 3<sup>rd</sup> international conference STESSA 2000*, Mazzolani F, Tremblay R (eds). Taylor & Francis: Montreal, Canada, 2000; 33–38.
23. Iwata M, Murai M. Buckling-restrained brace using steel mortar planks; performance evaluation as a hysteretic damper. *Earthquake Engineering and Structural Dynamics* 2006; **35**:1807–1826.
24. Merritt S, Uang CM, Benzoni G. Subassemblage Testing of CoreBrace Buckling Restrained Braces. *Structural Systems Research Project, Report No. TR-2003/01*, University of California, San Diego, 2003.
25. Merritt S, Uang CM, Benzoni G. Subassemblage Testing of Star Seismic Buckling Restrained Braces. *Structural Systems Research Project, Report No. TR-2003/04*, University of California, San Diego, 2003.
26. Newell J, Uang CM, Benzoni G. Subassemblage testing of corebrace buckling restrained braces (G series). *Structural Systems Research Project, Report No. TR-2006/01*, University of California, San Diego, 2006.
27. Usami T, Kasai A, Kato M. Behavior of buckling-restrained brace members. *Behavior of steel structures in seismic areas, Proceedings of the 4<sup>th</sup> international conference STESSA 2003*, Mazzolani F (ed.). A.A. Balkema Publishers: Naples, Italy, 2003; 211–216.
28. Zhao J, Wu B, Ou J. A novel type of angle steel buckling-restrained brace: Cyclic behavior and failure mechanism. *Earthquake Engineering and Structural Dynamics* 2011; **40**:1083–1102.
29. Takeuchi T, Ida M, Yamada S, Suzuki K. Estimation of cumulative deformation capacity of buckling restrained braces. *Journal of Structural Engineering (ASCE)* 2008; **134**(5):822–831.
30. Andrews BM, Fahnestock LA, Song J. Ductility capacity models for buckling-restrained braces. *Journal of Constructional Steel Research* 2009; **65**:1712–1720.
31. Tsai KC, Hsiao PC. Pseudo-dynamic test of a full-scale CFT/BRB frame Part II: Seismic performance of buckling-restrained braces and connections. *Earthquake Engineering and Structural Dynamics* 2008; **37**:1099–1115.
32. CEN. *EuroCode 3: Design of steel structures – Part 1–1: General rules and rules for buildings*, ENV 1993-1-1. European Committee for Standardization: Bruxelles, 2005.
33. Mazzoni S, McKenna F, Scott, MH, Fenves GL, et al. *OpenSees Command Language Manual*. Pacific Earthquake Engineering Research Center: Berkeley, 2007.
34. Somerville PG, Smith NF, Punyamurthula S, Sun JI. Development of ground motion time histories for phase 2 of the FEMA/Sac steel project. SAC Background Document. Report No. SAC/BD-99-03, SAC Joint Venture, 555 University Ave., Sacramento, 1997.
35. MacRae GA, Kimura Y, Roeder C. Effect of Column stiffness on Braced Frame Seismic Behaviour. *Journal of Structural Engineering (ASCE)* 2004; **130**(3):381–391.
36. Tremblay R. Achieving a stable inelastic seismic response for multi-story concentrically braced steel frames. *Engineering Journal AISC* 2003; **40**:111–129.
37. CEN. *EuroCode 8: Design of structures for earthquake resistance – Part 3: Assessment and retrofitting of buildings*. European Committee for Standardization: Bruxelles, 2005.
38. Marino EM, Nakashima M. Seismic performance and new design procedure for chevron-braced frames. *Earthquake Engineering and Structural Dynamics* 2006; **35**:433–452.
39. Bosco M, Rossi PP. Seismic behaviour of eccentrically braced frames. *Engineering Structures* 2009; **31**:664–674.
40. Rossi PP, Lombardo A. Influence of the link overstrength factor on the seismic behaviour of eccentrically braced frames. *Journal of Constructional Steel Research* 2007; **63**(11):1529–1545.